# Map-Guided Approach for the Automatic Detection on Landsat TM Images of Forest Stands Damaged by the Spruce Budworm

**Stéphane Chalifoux, François Cavayas, and James T. Gray**

## Abstract

*A map-guided approach was followed in order to identify forest stands damaged by the spruce budworm on Landsat TM images. Pixels included in each forest polygon as indicated on the map are extracted and their values in TM4 and TM5 spectral bands, transformed to reflectance units, are analyzed using a set of numeric rules. These rules are based on the frequencies of occurrence of pixel values in pre-defined intervals. The change-detection/identification accuracy varies according to the stand type. Thus, for coniferous stands with defoliation and/or light mortality, the accuracy was 95 percent whereas, for mixed stands, an accuracy lower than 80 percent was obtained. These results indicate that the proposed method behaves well as a fast detection technique in a complex forest environment. It has a definite advantage over all standard methods, by permitting the characterization as damaged or not of an entire stand, instead of the individual image pixel. Ways to further improve its performance, especially in the case of mixed stands, are also discussed.*

## Introduction

Many factors could drastically modify the structure and the composition of the forest cover. Such factors are insect epidemics, forest cutting, wind throws, and fire. The efficient inventory of these changes on a regular basis is a fundamental operation of any forest management system. This is particularly true for the Province of Quebec, Canada, where forests cover more than 1 million km$^2$. Digital satellite imagery, significantly improved in terms of spatial, spectral, and radiometric resolutions in the last decade, with its synoptic and repetitive view, provides good potential for automatic forest-cover change detection and map updating.

Research on computer analysis of satellite imagery, however, based mostly on a pixel-by-pixel supervised classification, has not yet led to a reliable methodology which could be applied on a routine basis for forestry map updating purposes (Gougeon, 1991). The potential of a new approach for change detection and forestry map updating has been evaluated at the Laboratory of Remote Sensing of the Université de Montréal. It is based on an automatic comparison of the existing forestry map with a more recent satellite image (map-guided approach). The map is used to segment the image into forest polygons. The pixels included in each polygon are then automatically identified and analyzed in order to detect radiometric anomalies which could be associated with a disturbance of the anticipated ground cover on the map. The application of this change-detection technique with a SPOT HRV multispectral image has given encouraging results (change-detection and identification accuracy of 87 percent) in searching for forest stands disturbed by various types of cutting (Cavayas and Francouer, 1991).

The objective of this paper is to describe an experiment conducted with this map-guided approach and Landsat TM imagery in order to detect forest stands damaged by the spruce budworm [*Choristoneura fumiferana* (Clem.)], whose periodic outbreaks severely affect balsam fir and white spruce in eastern Canada. Three outbreaks of this budworm occurred in the present century (Ahern *et al.*, 1986) with the last one commencing at the end of the sixties. In the Province of Quebec the epidemic was still creating havoc in some regions, such as the study site in Forillon National Park, well into the eighties (Godard *et al.*, 1990).

## Literature Review

### Potential Use of the Satellite Imagery

To make decisions and efficiently manage the forests, the inventory of insect damage has to be made at various scales, from individual trees up to forest stands. The estimation of the number of damaged trees using present day satellite imagery is difficult, if not impossible. Even with imagery of much better resolution such as aerial color-infrared photography, the detection of individual damaged trees may be problematic (Klein, 1982; Murtha and Fournier, 1992). Only estimates of loss in leaf biomass due to defoliation seems to be possible, but with variable accuracy depending on the damage severity (Hudak *et al.*, 1993).

On the scale of forest stands, the objective of an inventory could be the detection of zones where the insect epidemic is currently manifesting itself. This could be useful in planning immediate action to stop the epidemic. For this inventory, sensors with spectral bands well adapted to the optical characteristics of damaged trees have to be used (Ahern *et al.*, 1986). For coniferous trees, these characteristics are the red-brown coloration of attacked trees ("red-attack"). Satellite imagery cannot be applied to this type of inventory on a regular basis for two principal reasons: (a) the "bio-window" when coniferous trees have this characteristic coloration is narrow (only a few weeks) and (b) the spectral bands and spatial resolution are not well adapted for this operation.

S. Chalifoux is with Tecsult Forestry Inc., 85, Ste-Catherine St. West, Montréal, Québec H2X 3P4, Canada.

F. Cavayas and J.T. Gray are with the Département de géographie, Université de Montréal, P.C. 6128, BO "Centre-Ville," Montreal H3C 3J7, Canada (cavayasf@ere.umontreal.ca).

Photogrammetric Engineering & Remote Sensing, Vol. 64, No. 6, June 1998, pp. 629–635.

0099-1112/98/6406–629$3.00/0

Sirois and Ahern (1988), for example, using SPOT HRV multispectral imagery for an area which was recently affected by the pine beetle, found that the minimum detectable surface area is approximately 1 to 2 ha in extent when 80 to 100 percent of the trees have a red crown. These authors suggest that such a limited spatial resolution is of little use in guiding epidemic control operations.

Satellite imagery is rather well adapted, however, to inventory of cumulative damage (previous year's defoliation and mortality) and to the updating of forestry maps (Sirois and Ahern, 1989). An indirect estimation of current year defoliation could also be made by comparing early and late summer images (Hudak *et al.*, 1993).

#### Methodologies of Information Extraction

The basic methodology followed in previous investigations was pixel-by-pixel supervised classification. For example, Godard *et al.* (1990) successfully classified pixels of a Landsat TM image covering the Gaspésie peninsula, Quebec, into various categories of defoliation (defoliation absent, light, moderate, and heavy). The forest cover was affected by the spruce budworm, and coniferous or deciduous dominated stands were considered. The classification accuracy per class using test sites ranged from 85 to 95 percent. In contrast, they obtained much lower accuracies in trying to classify a SPOT HRV multispectral image of the same area and with the same stratification. They attribute this difference, in favor of the TM image, to the use of the TM5 band and the greater dynamic range of the TM bands compared to the equivalent SPOT HRV bands. Hudak *et al.* (1993) obtained much better accuracies in classifying pixels of SPOT HRV covering coniferous forest in eastern Canada damaged by the eastern hemlock looper. Using a stratification similar to that of Godard *et al.* (1990), they obtained a classification accuracy ranging from 75 percent (light defoliation) to 100 percent (moderate and severe defoliation). Using Landsat TM of another area for classifying pixels damaged by the same insect, they obtained an accuracy per defoliation class ranging from 93 percent (light defoliation) to 100 percent (moderate defoliation). However, the accuracy with Landsat TM was lower (from 71 percent to 89 percent) in identifying severity of damage caused by another insect, the blackheaded budworm.

These results confirm the potential of satellite imagery, especially that of Landsat TM, for mapping cumulative defoliation and mortality of coniferous trees. However, it seems that classification results vary according to the stand composition, and the spatial pattern and extent of the damage. A more uniform area in terms of stand composition and patterns of epidemic could favor better results than an area with more variable composition and/or complex epidemic spatial patterns. Concerning the stand composition, Ekstrand (1994) notes that the identification on Landsat TM images of rather moderately defoliated Norway spruce stands could be impossible if hardwoods and pines are present within the spruce stands. Contrast variations due to atmospheric and topographic effects and reflectance variations due to different stand architectures could also give rise to variable classification results.

The major problem, however, with this method is that the obtained results cannot be directly used in a forest-map updating operation because the identification unit is not an entire stand but the individual pixel. To take one example, a stand is lightly damaged not because every contiguous pixel in it has been equally affected by the insect, but because the proportion of damaged trees within a stand is between some pre-specified limits, e.g., 1 percent to 30 percent. The processing operation will tend to show a patchwork quilt effect whereby the stand boundaries will not be easily recognizable. The same problem is also present in the case of change detection by post-classification comparison of multi-date satellite images, even if sophisticated methods of comparison are used (Gougeon, 1991).

An alternative to per-pixel classification is image segmentation in zones which could be assigned to particular stands and, after this, the classification of each segment. Segmentation methods, however, as applied to satellite images of forested territories are rather inefficient because forest stands do not have sharp spectral limits and texture is not a major discriminant characteristic at the satellite image scale (St-Onge and Cavayas, 1995).

The change detection technique proposed in this paper uses an existing forestry map to provide the desired limits of forest stands. The analysis could then be focused within these limits to detect eventual changes (Cavayas and Francoeur, 1991). It is to be noted that this map-guided approach was also proposed by other authors in a forestry inventory context with satellite imagery but with different objectives. For example, Goodenough (1988) uses existing maps as an assistance in choosing meaningful training sites for pixel-by-pixel supervised classification and Ekstrand (1994) employs this approach to adjust coefficients of a linear transformation of TM4 values to degree of defoliation of Norway spruce stands.

## Study Area and Data Sets

Forillon National Park is located in the central part of the Gaspésie peninsula, Quebec (Figure 1). The dominant forest species are balsam fir, black spruce, and white birch. A Landsat-5 TM image acquired on 22 July 1986 was used in this study. This image was geometrically corrected to the UTM grid and resampled by cubic convolution at a 25-m spatial resolution. This acquisition date was chosen for compatibility with the corresponding forestry map sheets at a scale of 1:20,000 (Quebec Forest Inventory Service). The latter were compiled using aerial photographs acquired at the same period as the satellite image. Thus, a good control basis for our method is provided. Color infrared aerial photographs at 1:15,000 scale, also acquired in 1986, were available and used for additional control. It is to be noted that in that year the epidemic was strongly in evidence in this region (Godard *et al.*, 1990). Only TM3, TM4, and TM5 bands were retained for this study. These bands are considered the best ones for a general purpose forest inventory (Horler and Ahern, 1986).

According to the stratification employed in the forestry map, two classes of epidemic due to the spruce budworm are recognized: light and severe epidemic. Light epidemic is considered as a stand disturbance factor and means that a proportion of coniferous trees within the stand are dead, but there is a high proportion of still living coniferous trees. These living trees may be defoliated or not. If the defoliated trees present a loss of needles not in excess of 50 percent, a light defoliation symbol is indicated on the map. When the defoliation exceeds 50 percent, heavy defoliation is indicated. If there is absence of mortality, the coniferous trees may be lightly or heavy defoliated. When almost an entire coniferous-dominated stand is killed by the epidemic, this is indicated as the origin of a new natural or planted stand (severe epidemic). Thus, the following forest classes could be present in coniferous or deciduous dominated stands:

- Stands with light defoliation
- Stands with heavy defoliation
- Stands with light mortality (light epidemic)
- Stands with light mortality and light defoliation
- Stands with light mortality and heavy defoliation
- Stands with severe mortality (severe epidemic)

## Image Preprocessing

In order to work with standardized units, digital counts in the various TM bands were transformed to reflectances after

corrections for atmospheric effects. For this transformation, a standard mid-latitude summer atmosphere was assumed. The aerosol optical depth during the satellite overpass was inferred using deep sea water located on the image as a dark target in conjunction with an atmospheric code (REFLECT software package: Cavayas *et al.*, in preparation). This code is the "6S" (Second Simulation of the Satellite Signal in the Solar Spectrum: Vermote *et al.*, 1997). The atmosphere was considered as horizontally uniform across the terrain and the aerosol of the same nature as over the sea. Topographic effects on image radiometry were ignored. The high sun elevation and the generally moderate relief of the area were not expected to alter significantly the radiance values of the forest cover, except in the TM4 and the TM5 spectral bands for stands located on a few steep slopes.

Once the atmospheric parameters were computed, the reflectance of each pixel was estimated (Lambertian assumption) using the following equations:

$$R_t^* = \frac{\pi(A_1 \cdot DC + A_0)}{T_{gas} \cdot E_s \cdot \cos Z}$$

$$R_t = \frac{(R_t^* - R_{atm})}{T_{down} \cdot T_{up} + s(R_t^* - R_{atm})}$$

Table 1 explains the parameters of the above equations and gives the values used in order to transform digital counts to reflectance units.

TABLE 1. TRANSFORMATION OF DIGITAL COUNTS TO GROUND REFLECTANCES: (A) LIST OF SYMBOLS; (B) VALUES OF ATMOSPHERIC AND ILLUMINATION PARAMETERS COMPUTED BY THE REFLECT SOFTWARE PACKAGE

**(a)**

| Symbol | Definition |
|---|---|
| $A_0$ | Calibration offset |
| $A_1$ | Calibration gain |
| $E_s$ | Solar exo-atmospheric irradiance adjusted for the earth-sun distance (W $m^{-2}$ $\mu m^{-1}$) |
| DC | Digital count |
| $R_{atm}$ | Atmospheric reflectance |
| $R_t$ | Target reflectance |
| $R_t^*$ | Target reflectance at the top of the atmosphere |
| s | Atmospheric spherical albedo |
| $T_{down}$ | Total (direct+diffuse) downward transmission of solar radiation due to atmospheric scattering |
| $T_{up}$ | Total (direct+diffuse) upward transmission of reflected radiation due to atmospheric scattering |
| $T_{gas}$ | Total (sun-target-sensor) gaseous transmission of solar radiation |
| Z | Solar zenith angle |

**(b)**

| Band | $A_0$* | $A_1$* | $E_s$ | $R_{atm}$ | s | $T_{gas}$ | $T_{down}$ | $T_{up}$ |
|---|---|---|---|---|---|---|---|---|
| TM3 | −1.20 | 0.806 | 1505.4 | 0.034 | 0.100 | 0.915 | 0.900 | 0.922 |
| TM4 | −1.50 | 0.815 | 934.2 | 0.018 | 0.066 | 0.959 | 0.927 | 0.944 |
| TM5 | −0.37 | 0.108 | 209.7 | 0.004 | 0.021 | 0.825 | 0.967 | 0.974 |

Solar zenith angle = 35.238°
*Source: *MOSAICS Technical Information Package*, Energy, Mines and Resources, Canada, Canada Centre for Remote Sensing, July 1987.

## Development of the Numeric Interpretation Key

### Image Segmentation

Earlier studies showed that maps compiled using conventional techniques may present significant differences in the location and shape of objects (contours of lakes, rivers, road network, forest polygons, etc.) when superimposed on satellite images (e.g., Goodenough, 1988; Goldberg *et al.*, 1988). In our case, a visual verification was made prior to the data analysis with the digitized contours of forest polygons superimposed on an enhanced color composite of TM3, TM4, and TM5 bands (Plate 1a). On this color composite (TM5, TM4, and TM3 in red, green, and blue, respectively), light green hues represent deciduous-dominated stands and dark green hues represent coniferous stands. The red-brown hues characterize stands damaged in various degrees by the spruce budworm. The fact that the map contours were established using aerial photography acquired in the same period as the satellite image simplified the verification of the image-map congruence.

The superimposition of polygon contours with this color composite (Plate 1a) showed that included pixels exhibit, in general, quite similar hue patterns for each forest class. Thus, it was admitted that congruence problems were virtually absent and that the segmentation of the image using the for-

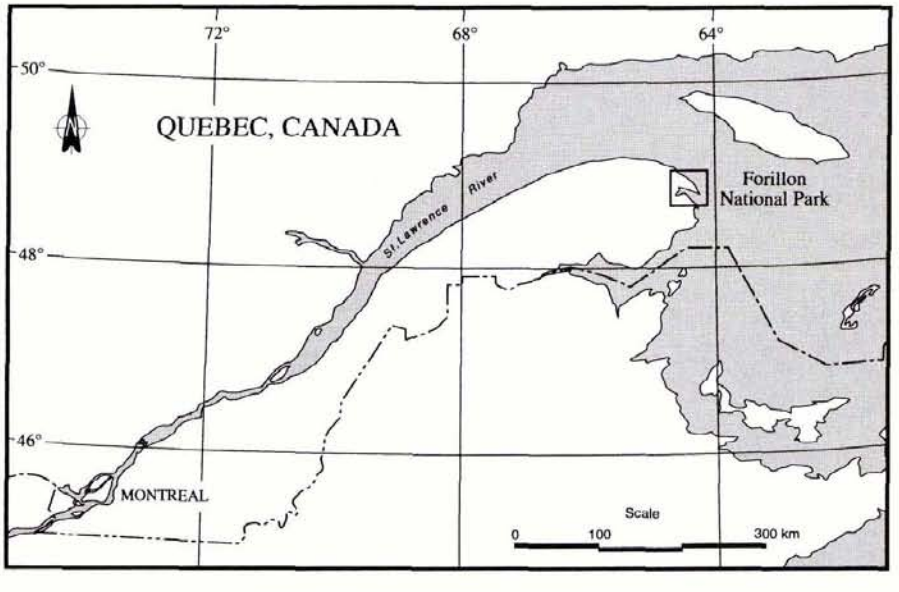


Figure 1. Location of the study site.

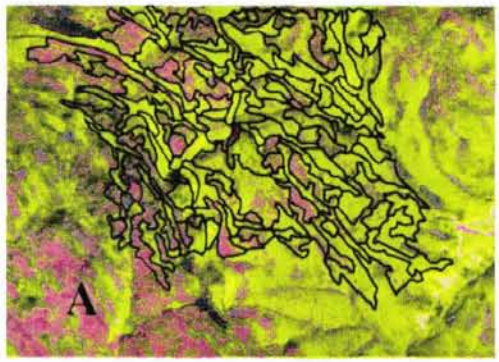


**a) Color composite**

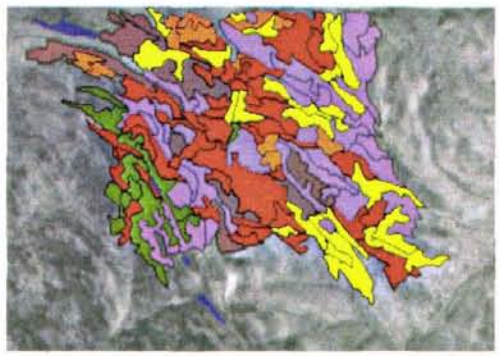

**Deciduous forest stand**
**Healthy mixed stand**
**Defoliated mixed stand**
**Healthy coniferous stand**
**Low defoliation in coniferous stand**
**High defoliation in coniferous stand**
**Heavy mortality in coniferous stand**

**b) Classified image**

Plate 1. (a) Digitized contours of forest polygons superimposed upon a false color composite (1:50,000 scale) of TM3, TM4, and TM5 bands; (b) Forest polygons classified using the proposed numeric key with TM4 band in background.

estry maps does not introduce significant bias in the analysis of pixel values.

#### Rules of the Numeric Interpretation Key

In the present study, no attempt has been made to develop a numeric interpretation key including rules for the discrimination of forest species, species associations, or forest-stand architectures. Our objective was to build a key which could be used in order to answer the question, "is the examined forest polygon damaged by the spruce budworm and, if the case arises, what is the damage severity?" Forest polygons within a 512- by 512-pixel subscene were used in order to develop the numeric key. These polygons were grouped first in three general categories: (1) coniferous, (2) mixed dominated by coniferous, and (3) mixed dominated by deciduous. For each category, the forest polygons were further grouped according to their degree of mortality and/or defoliation (Table 2), and their reflectance values were analyzed.

The reflectance values of forest stands did not show significant variations in the TM3 band according to the degree of damage by the spruce budworm. In fact, these values covered a small range from about 1.5 percent to 4.0 percent. Thus, it was decided to retain only the TM4 and TM5 spectral bands for further analysis.

Figure 2 shows the statistics of forest polygons in the TM4 and TM5 bands. The reflectances in the TM4 band cover a large interval, from about 20 percent to 40 percent or even more (Figure 2a). The high reflectance values of coniferous stands could be explained by the nature of the stands (rather sparse canopies with no tall trees). On the average, reflectances of coniferous stands present a slight decrease according to the severity of the damage. Canopies which are heavily touched by the epidemic (Figure 2a, classes C5 and C7) present in contrast a slight increase. This could be explained by the fact that the understory (composed mostly of deciduous shrubs, as indicated by color infrared photographs) is more visible to the sensor, thus causing increased reflectance in this band. The same trend was also observed by Ahern *et al.* (1991) in a similar forested environment affected by the spruce budworm. Mixed stands (either deciduous or coniferous dominated) show slightly higher average values than the coniferous stands. No clear trend, related to the severity of mortality and/or defoliation, is observed.

The reflectances in the TM5 band (Figure 2b) present lower differences according to the stand composition when compared to the TM4 band. In the case of mixed stands dominated by coniferous species, a slight increase in the average reflectance values with damage severity is observable. A closer examination of the histograms of individual stands in this band, however, has revealed that the distribution of pixel values follows some distinctive patterns according to the damage severity by the spruce budworm. Usually, the bulk of the reflectance values were within some characteristic intervals (Figure 3). Using as a criterion the frequencies of occurrence of pixel values within these specific intervals, it

TABLE 2. FOREST POLYGONS USED TO DEVELOP THE NUMERIC INTERPRETATION KEY

| Class | Symbol | Number of Polygons | Number of Pixels |
|---|---|---|---|
| *Coniferous* | | | |
| Healthy | C1 | 24 | 4160 |
| Lightly defoliated | C2 | 16 | 5671 |
| Heavily defoliated | C3 | 2 | 657 |
| Light mortality | C4 | 38 | 11908 |
| Light mortality and light defoliation | C5 | 12 | 3896 |
| Light mortality and heavy defoliation | C6 | NA | NA |
| Severe epidemic | C7 | 38 | 15473 |
| *Mixed (Coniferous)* | | | |
| Healthy | MC1 | 25 | 5006 |
| Lightly defoliated | MC2 | 11 | 3262 |
| Heavily defoliated | MC3 | 2 | 1110 |
| Light mortality | MC4 | 2 | 352 |
| Light mortality and light defoliation | MC5 | 17 | 8957 |
| Light mortality and heavy defoliation | MC6 | 8 | 2869 |
| *Mixed (Deciduous)* | | | |
| Healthy or lightly defoliated | MD12 | 65 | 57013 |
| Heavily defoliated | MD3 | 21 | 6036 |
| Light mortality | MD4 | 1 | 26 |
| Light mortality and light defoliation | MD5 | 33 | 14456 |
| Light mortality and heavy defoliation | MD6 | 14 | 6659 |

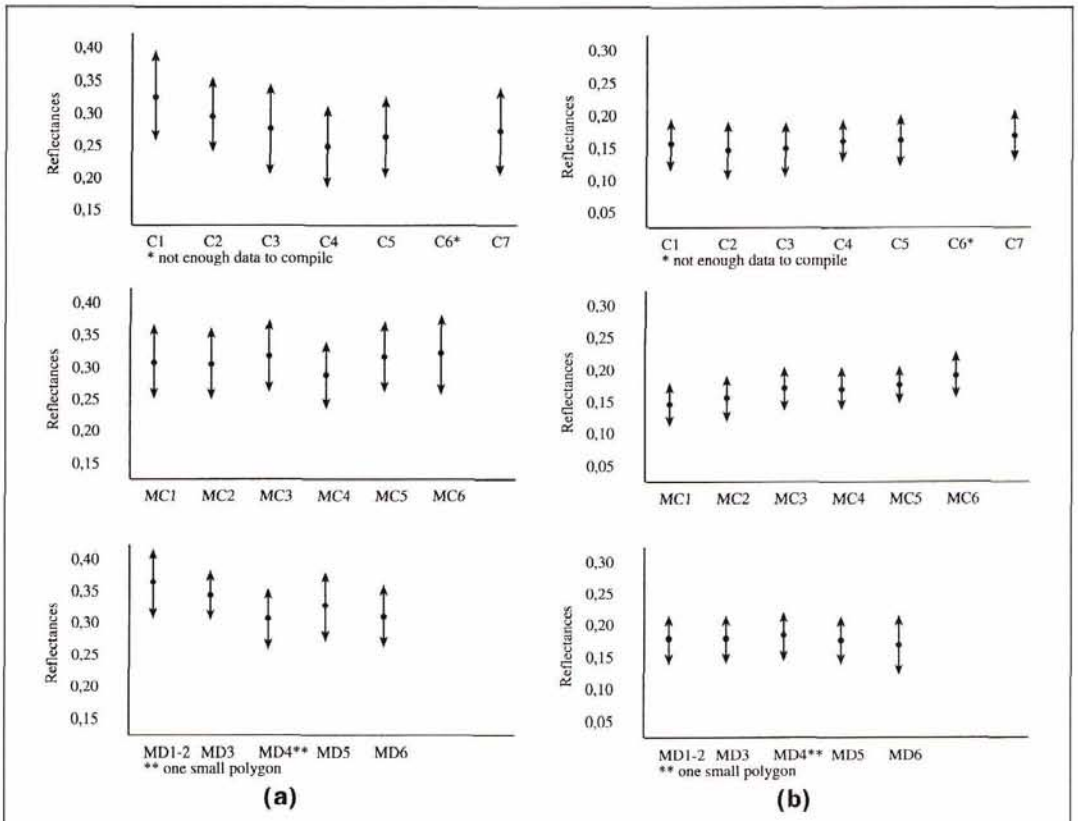


Figure 2. Statistics per forest class, error bars are ±1 standard deviation (see Table 2): (a) TM4 band, (b) TM5 band.

was possible to differentiate between four categories of coniferous stands according to the damage severity due to the spruce budworm (Figure 3a): healthy stand, lightly defoliated stand, highly defoliated stand, and stands with heavy mortality. No distinction was possible between defoliation and light mortality. For the mixed stands, dominated either by coniferous or deciduous species, only two classes could be distinguished (Figure 3b): healthy mixed stands and heavily defoliated (with or without light mortality).

Table 3 presents the histogram features in the TM4 and TM5 bands finally retained for the development of the numeric key. In this key, the TM4 band is used as a filter to allow the choice of the appropriate rules, including TM5 features for the detection of eventual damage within a stand. The great variance of the reflectance values in the TM4 band and the absence of clear trends associated with the budworm damage severity did not permit the more extensive use of this band. Features 1 and 2 in Table 3 are used to verify if the forest polygon is coniferous dominated. The mean value of TM4 (feature 3) is used in the case when the values of features 1 and 2 do not permit a definite decision. Features 4 to 10 in this table are used to detect defoliation levels using TM5 histograms. Feature 4 is used to detect healthy coniferous stands. Features 5 and 6 allow the identification of lightly defoliated coniferous stands. Features 7 and 8 allow the distinction between heavily defoliated stands and those with heavy mortality. Feature 9 is used to detect heavy defoliation within a mixed stand. Finally, the mean of the reflectance values in the TM5 band (feature 10) helps to make decisions in cases where the use of features 5 and 6 or 7 and 8 is not sufficient. Figure 4 shows how the features of Table 3 are used to make a decision about the presence of a damage and its severity.

## Application and Results

One-hundred seven forest polygons, located in a different sub-scene from that of the previous section, were used for testing the performance of this numeric interpretation key (Plate 1a). Seventy-one polygons were covered by mixed

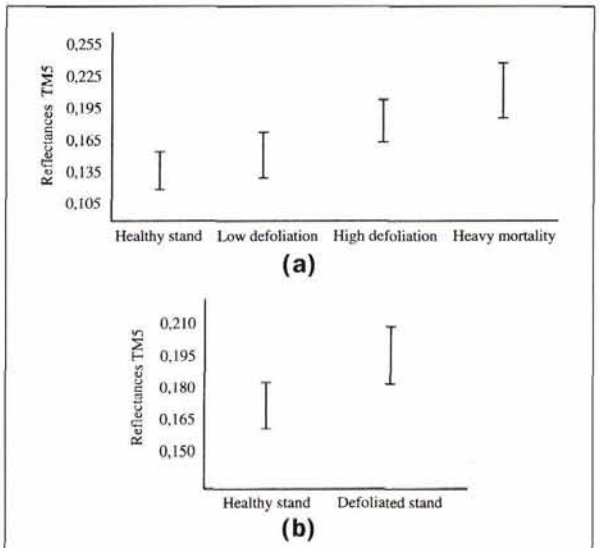


Figure 3. Characteristic intervals of reflectance values in TM5 band according to the spruce budworm damage: (a) mixed stands; (b) coniferous stands.

stands and 36 by coniferous stands. Plate 1b presents the classification obtained using this key and Tables 4a and 4b show the classification accuracy. In Table 4a, in 25 percent of cases the key was not able to act as a good filter for coniferous stands. The complexity of the epidemic patterns and forest composition could explain this. For example, as already mentioned, the sensitivity of the TM4 band to the understory vegetation in severely attacked coniferous stands could give rise to spectral similarity to mixed stands. To improve the performance of the key at this level, the use of the indicated polygon label on the map could be a valuable solution.

Using the characteristic histogram features of the TM5 band, the overall classification mean accuracy was 76 percent (Table 4b). It is to be noted that in this table the coniferous stands lightly and heavily defoliated were grouped because of the low number of polygons examined in either class. The best classification accuracy was obtained for coniferous stands with partial mortality and/or defoliation (95 percent) and the worst for mixed stands either healthy or damaged (69 percent and 77 percent, respectively). Finally, stands with heavy mortality were detected with 64 percent accuracy. But, if one considers that in 29 percent of the cases the polygons were classed as defoliated stands, this indicates a good ability to detect, in general, damaged stands. In fact, by grouping all the polygons representing damaged stands (mixed, coniferous, and those with heavy mortality), the damage-detection accuracy is on the order of 85 percent. With the optimization of the TM4 filter, a better overall performance of the key could be expected. Another possibility for an optimization of the key, in the case of mixed stands, is the distinction between mixed with coniferous dominance and mixed with deciduous dominance. As is shown in Figure 2, mixed stands present different behavior according to the dominant species.

TABLE 3. FEATURES (DECISION RULES) USED IN THE NUMERIC KEY

**TM4 Band**

1. Relative frequencies in the range of reflectances: 26-30%;
2. Relative frequencies in the range of reflectances: 35-38%;
3. Mean;

**TM5 Band**

4. Relative frequencies in the range of reflectances: 11-13%;
5. Relative frequencies in the range of reflectances: 13-15%;
6. Relative frequencies in the range of reflectances: 15-18%;
7. Relative frequencies in the range of reflectances: 16,5-18%;
8. Relative frequencies in the range of reflectances: 19,5-21%
9. Cumulative frequencies of reflectance value: 18%;
10. Mean.

## Discussion and Future Developments

The obtained results show that the proposed method behaves well in a very complex forestry context, and the accuracy attained is adequate for a fast and efficient change detection of damaged forest stands using TM imagery. The use of the method, however, in a forestry map updating context is problematic. Even in the case of coniferous stands where the best change-detection accuracy was obtained, a question remains open: how to make the distinction between mortality and defoliation as requested by the forest inventory guidelines. For

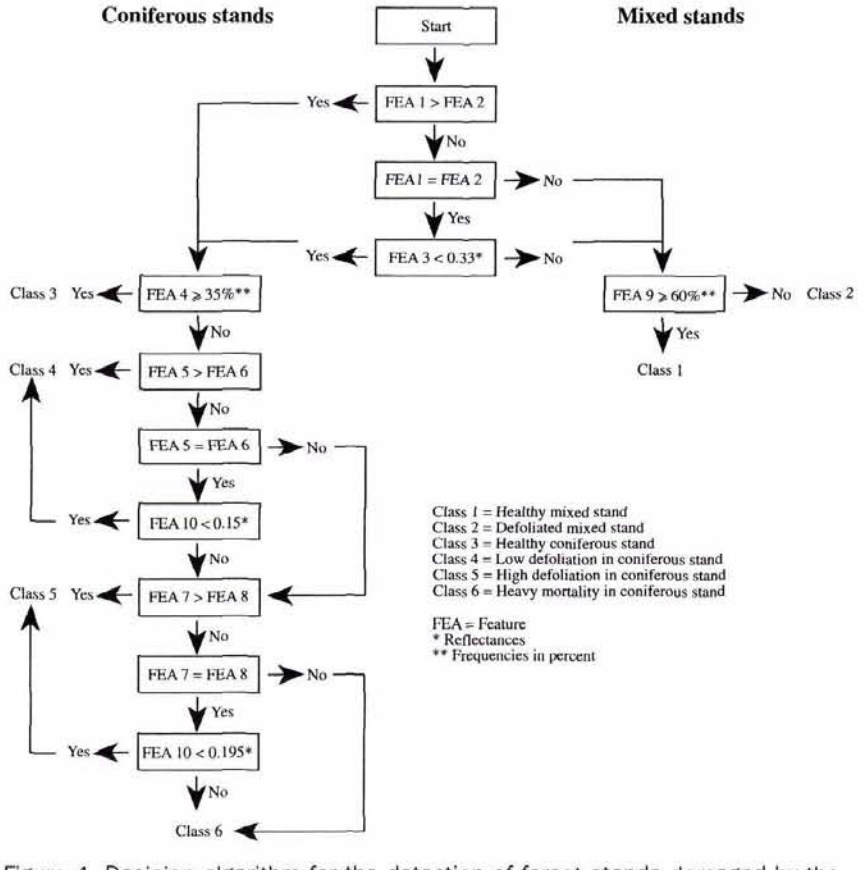


Figure 4. Decision algorithm for the detection of forest stands damaged by the spruce budworm.

TABLE 4a. PERFORMANCE OF THE TM4 BAND FILTER

| | Mixed Stands | Coniferous Stands | Polygon Counts |
|---|---|---|---|
| Mixed Stands | 92% | 8% | 71 |
| Coniferous Stands | 25% | 75% | 36 |

Mean accuracy = 84%

TABLE 4b. DETECTION AND IDENTIFICATION ACCURACY OF DAMAGED AND UNDAMAGED STANDS

| | Healthy Stands | Defoliated Stands | Stands with Heavy Mortality | Polygon Counts |
|---|---|---|---|---|
| Healthy Mixed Stands | 69% | 28% | 3% | 36 |
| Defoliated Mixed Stands | 23% | 77% | 0% | 35 |
| Healthy Coniferous Stands | — | — | — | 3* |
| Defoliated Coniferous Stands | 5% | 95% | 0% | 19 |
| Stands with Heavy Mortality | 7% | 29% | 64% | 14 |

*not enough data to compile Mean accuracy = 76%

comparison with our method, a supervised classification was performed using forest polygons as training sites in the manner proposed by Goodenough (1988) with various grouping schemes to construct forest classes. The mean classification accuracy was much lower (not better than 50 percent) from that obtained in the present study.

To optimize the use of the proposed key, either as a fast change-detection technique or as a tool for forestry map updating purposes, the following aspects have to be examined in the future:

- the behavior of the key in other forested territories with different species distribution and spatial patterns of the epidemic;
- the behavior of the key in the case where various types of disturbance are simultaneously present, for example, defoliation, forest cuttings, and wind throws;
- the eventual use of other TM bands or derived images such as the NDVI (vegetation index; Chalifoux *et al.*, 1993); and
- the possibility of taking into account the presence of an understory which influences the results in the case of low density canopies or those which have been severely damaged. The use of the forestry polygon label indicating the anticipated density of the forest stand could constitute the basic element of an eventual solution to this problem.

## Conclusions

The change detection method proposed in this paper has two major advantages compared to methods employing statistical classification on a pixel-by-pixel basis:

- In the first place, an entire stand is characterized as damaged or undamaged; this is much closer to the forest inventory approach than is classification of individual pixels which characterize the class of a particular pixel but not that of a forest stand.
- In the second place, forest polygons could be further classified according to the damage severity.

Concerning this latter aspect, the results presented here are admittedly qualitative in nature as used in forestry inventory techniques. A more quantitative characterization is possible using techniques such as those suggested by Ekstrand (1994). The fact that the analysis could be made at a local level within the limits of a particular stand should certainly facilitate the application of such techniques. A further refinement of our method could be the inclusion of the forest-stand density as indicated on the existing map. In the present case, this variable has not been taken into account in grouping our polygons into defoliation and/or mortality classes.

## References


Ahern, F.J., W.J. Bennett, and E.G. Kettela, 1986. An initial evaluation of two digital airborne imagers for surveying spruce budworm defoliation, *Photogrammetic Engineering & Remote Sensing*, 52(10):1647–1654.

Ahern, F.J., T. Erdle, D.A. Maclean, and I.D. Kneppeck, 1991. A quantitative relationship between forest growth rates and Thematic and Mapper reflectance measurements, *International Journal of Remote Sensing*, 12(3):387–400.

Cavayas, F., M. Beaulieu, and P.M. Teillet, in preparation. Atmospheric and topographic effects correction on satellite imagery using the REFLECT software.

Cavayas, F., and A. Francoeur, 1991. Système expert pour la mise à jour des cartes forestières à partir des images satellites, *Télédétection et Gestion des Ressources*, Vol. VII (P. Gagnon, editor), L'Association Québécoise de Télédétection, Québec, pp. 170–178.

Chalifoux, S., F. Cavayas, and J. Gray, 1993. Suivi de la ressource forestière à l'aide des images satellites, *S.I.G. et Environnement, Les Dossiers de la Revue de Géographie Alpine*, No 9, 1993, Institut de Géographie Alpine, Université Joseph Fourier, Grenoble, France, pp. 53–57.

Ekstrand, S., 1994. Assessment of forest damage with Landsat TM: Correction for varying forest stand characteristics, *Remote Sensing of Environment*, 47(3):291–302.

Goldberg, M., D.G. Goodenough, and G. Plunket, 1988. A knowledge-based approach for evaluating forestry-map congruence with remotely sensed imagery, *Phil. Trans. R. Soc. Lond.*, A 324:447–456.

Godard, M., J. Gray, and J. Poitevin, 1990. The relative merits of SPOT HRV and Landsat TM images for forest cover change detection in Forillon National Park, Québec, Canada, *IEEE Transactions on Geoscience and Remote Sensing*, 28(4):745–746.

Goodenough, D.G., 1988. Thematic Mapper and SPOT integration with Geographic information system, *Photogrammetric Engineering & Remote Sensing*, 54(2):167–176.

Gougeon, F., 1991. *A Forestry Expert Package — The Lake Traverse Study*, Information Report PI-X-108, Petawawa National Forestry Institute, Forestry Canada, 16 p.

Horler, D.N.H., and F.J. Ahern, 1986. Forestry information content of Thematic Mapper data, *International Journal of Remote Sensing*, 7(3):405–428.

Hudak, J., S.E. Franklin, and J.E. LuDher, 1993. Detection and classification of forest damage using remote sensing, *Proc. of the International Forum on Airborne Multispectral Scanning for Forestry and Mapping*, Quebec Canada, April 1992 (D.G. Leckie and M.D. Gillis, editors), Information Report PI-X-113, Petawawa National Forestry Institute, Forestry Canada, pp. 36–43.

Klein, W.H., 1982. Estimating bark beetle-killed lodgepole pine with high altitude panoramic photography, *Photogrammetric Engineering & Remote Sensing*, 48(5):733–737.

Murtha, P.A., and R.A. Fournier, 1992. Varying reflectance patterns influence photo interpretation of dead tree crowns, *Canadian Journal of Remote Sensing*, 18(3):167–173.

Sirois, J., and F.J. Ahern, 1988. An investigation of SPOT HRV for detecting recent mountain pine beetle mortality, *Canadian Journal of Remote Sensing*, 14(2):104–108.

St-Onge, B., and F. Cavayas, 1995. Estimating forest stand structure from high resolution imagery using the directional variogram, *International Journal of Remote Sensing*, 16(11):1999–2021.

Vermote, E., D. Tanré, J.L. Deuzé, M. Herman, and J.J. Morcrette, 1997. Second simulation of the satellite signal in the solar spectrum, 6S: An overview, *IEEE Transactions on Geoscience and Remote Sensing*, 35(3):675–686.


(Received 13 May 1996; revised and accepted 26 September 1997; revised 11 November 1997)